J Therm Anal Calorim (2016) 126:467–471
DOI 10.1007/s10973-016-5567-7

Thermal hazard assessment of 4,10-dinitro-2,6,8,12-tetraoxa-4,10-diazaisowutrzitane (TEX) by accelerating rate calorimeter (ARC)

Guangyuan Zhang[1,2] · Shaohua Jin[1] · Lijie Li[1] · Yunkai Li[1] · Deqiu Wang[2] · Wei Li[2] · Ting Zhang[1] · Qinghai Shu[1]

Received: 10 January 2016 / Accepted: 14 May 2016

Abstract The thermal decomposition behaviors of 4,10-dinitro-2,6,8,12-tetraoxa-4,10-diazaisowutrzitane (TEX) were studied by using accelerating rate calorimetry to achieve the hazard assessment of TEX explosive, and the kinetic parameters were studied from the measured self-heating rate data by assuming a zero-order reaction. Moreover, the specific heat capacity date of TEX was obtained from differential scanning calorimetry. These results could be contributed to improve the safety in the reaction, transportation, and storage processes of TEX.

Keywords TEX · Thermal stability · Accelerating rate calorimetry (ARC) · Explosive

Abbreviations

Φ	Thermal inertia factor
T_0/°C	Initial self-heat temperature
T_f/°C	Final decomposition temperature
ΔT_{ad}/°C	Adiabatic temperature rise
m_0/°C min^{-1}	Initial temperature rise rate
m_m/°C min^{-1}	Maximum temperature rise rate
T_m/°C	Temperature of maximum temperature rise rate
Θ_m/min	Time of maximum temperature rise rate
E_a/kJ mol^{-1}	The apparent activation energy
R	The gas constant
A	Pre-exponential factor

Introduction

Currently, explosives with superior detonation characteristics and/or decreased sensitivity to exterior stimuli [1–12] are of great concern. 4,10-dinitro-2,6,8,12-tetraoxa-4,10-diazaisowutrzitane, also called as TEX (Fig. 1), is a promising insensitive explosive [13–17] with high detonation velocity similar to RDX and HMX with excellent insensitivities toward mechanical and thermal stimuli comparable to NTO (see Table 1).

Though the thermal behavior and safety of TEX [14, 22] have been studied by both theoretically and experimentally, the explosion hazard of TEX is desired to be focused on the investigation of its thermal hazardous, especially under adiabatic conditions, which helps developing a thorough understanding of the potential thermal hazards relating to their safe manufacturing, handling and storage.

In this paper, the thermal explosion hazard and adiabatic decomposition progress of TEX were investigated by accelerating rate calorimeter (ARC) to acquire thermodynamic parameters for self-heat reactions. In addition, the self-accelerating decomposition temperature, the adiabatic decomposition temperature rise and the adiabatic time to explosion were also obtained as well, which would provide helpful information for its manufacturing and applications.

✉ Qinghai Shu
qhshu121@bit.edu.cn

[1] School of Materials Science and Engineering, Beijing Institute of Technology, Beijing 100081, People's Republic of China

[2] Gansu Yinguang Chemical Industry Group Co., LTD, Baiyin 730900, Gansu, People's Republic of China

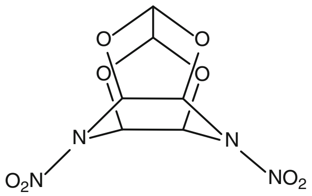

Fig. 1 Molecular structure of TEX

Table 1 Detonation properties of TEX in comparison with other commonly used high-energy explosives

	ρ/g cm^{-3}	D/m s^{-1}	P/Gpa	Fs/Ib	Is/cm	Dec./°C
TEX [18]	1.99	8665	37.49	>64	>116	304.0
RDX [19]	1.82	8802	36.43	63	55.88	240.2
HMX [20]	1.90	9046	39.78	63	73.66	282.1
NTO [21]	1.91	8120	31.11	79	>280	273.9

Experimental

Materials

The sample (TEX) investigated was purchased from Gansu Yinguang Chemical Industry Group Co., LTD., purity 99.70 %. Element analysis: C% 27.66 (27.49 % calculated), N% 20.78 % (21.37 % calculated), O% 49.21 % (48.83 % calculated), H% 2.35 (2.31 % calculated).

Apparatus and test conditions

Elemental analyses are determined on a Vario EL cube elemental analyzer. ARC has been used widely for estimating the explosion characteristics of explosives [23–27]. In this study, a NETZSCH Co., Ltd accelerating rate calorimeter (ARC) using a 1/4-in. Hastelloy bomb with a thermocouple clip located on the bottom of the bomb was used.

Generally, when measuring one ARC test, the sample is placed in a Hastelloy bomb, sealed with air atmosphere, initially heated to 70 °C, and then equilibrated for 30 min, followed by a 10-min seek for an exothermic signal, which can be detected if the self-heat rate (SHR) is over 0.02 °C min^{-1}. Then, the temperature will be increased by 5 °C with the subsequent repetition of the heat–wait–seek (H–W–S) periods until the exothermic signal is detected.

Data of sample and bomb in the experiment are listed in Table 2. To ascertain the accuracy of measurement, the instrument was calibrated and then verified using 20 mass% di-tertiary-butyl peroxide (DTBP, >98 %) 80 mass% toluene solution before the experiments.

Results and discussion

The specific heat capacity of TEX

Figure 2 showed the specific heat capacity of TEX as a function of temperature using differential scanning calorimetry (DSC). The sample mass was 25.6 mg, and the heating rate was 10 °C min^{-1} from 5 to 35 °C. In determined temperature range, specific heat capacity of TEX presented a good linear relationship with temperature, and the linear correlation coefficient is 0.9986. The equation describing the relationship can be written as $C_p = 0.81806 + 0.00341 \times \mathrm{T}$, $5.0\ ^\circ\mathrm{C} \le T \le 35\ ^\circ\mathrm{C}$. The resulted molar specific heat capacity of TEX is therefore calculated as 0.9038 J g^{-1} K^{-1} at 298.15 K.

Data analysis

The measured data and curves of test for TEX are given in Figs. 3–5 and Table 3. Figure 3 shows temperature and pressure versus time for TEX in the heat–wait search operational logic of the ARC test, revealing that after five H–W–S periods, the self-decomposition reaction of DNTF started to take place at 215.8 °C and lasted for 984.2 min, during which the temperature and pressure in the reaction system increased abruptly at the rate approximately 274.6 min^{-1} and 5748 kPa min^{-1}, respectively. This indicated that the decomposition reaction released enormous energy and could cause a disaster when occurred uncontrolled in a closed vessel.

As shown in Fig. 3, the self-heat rate (SHR) of TEX decomposition raised slowly when the reaction temperature

Table 2 Data of samples and sample bomb

Sample mass/Ms g^{-1}	Bomb mass/Mb g^{-1}	Test cell type	Φ	Temperature range/°C
0.132	21.03	Hastelloy	75.03	180–350
0.137	21.03	Hastelloy	72.33	190–320

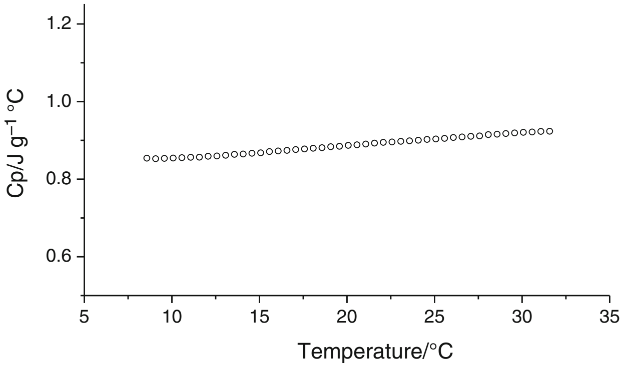

Fig. 2 Specific heat capacity of TEX as a function of temperature

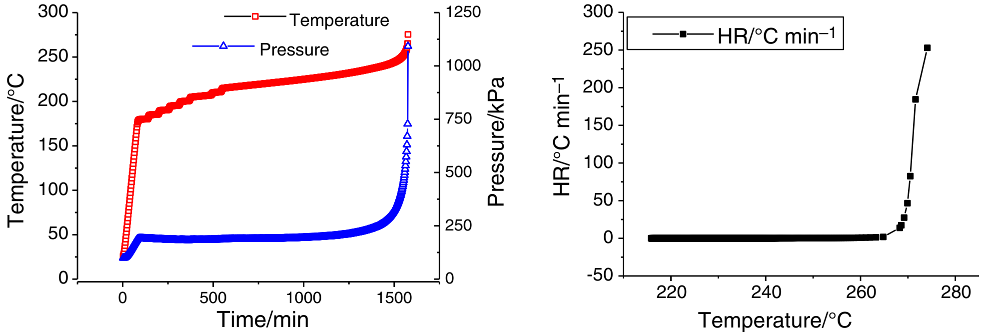

Fig. 3 Temperature and pressure versus time (*left*) and self-heat rate versus temperature (*right*)

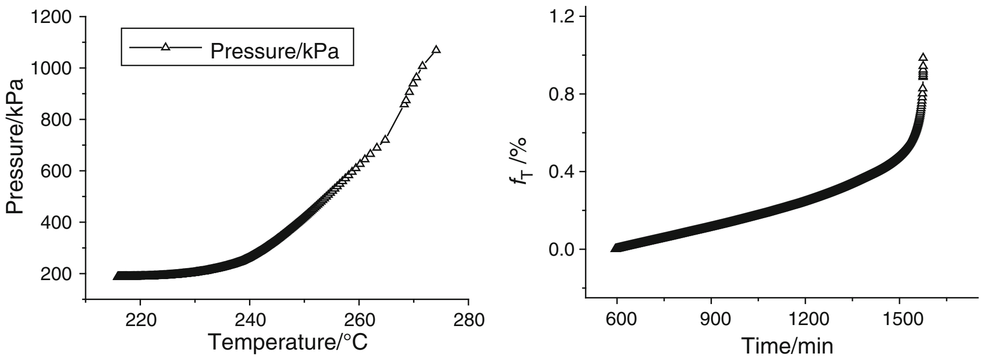

Fig. 4 Pressure versus temperature (*left*) and temperature conversion rate versus time

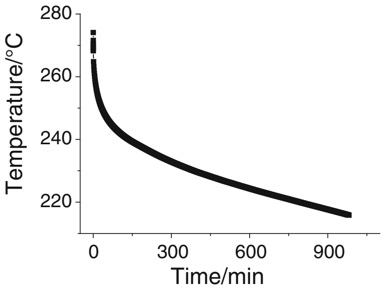

Fig. 5 Time to reach maximum temperature rise rate (TMR) versus temperature

Table 3 Thermal decomposition parameters of TEX by ARC

Parameters	Measured data	Corrected data
T_0/°C	215.8	210.48
T_f/°C	274.9	4644.76
ΔT_{ad}/°C	59.1	4434.27
m_0/°C min^{-1}	0.02	1.50
m_m/°C min^{-1}	255.10	19,140.15
T_m/°C	274.6	4622.25
θ_m/min	984.2	13.12
H/J g^{-1}	4363.40	

was below 267 °C, while a runway reaction was found when the reaction temperature exceeded 267 °C along with the significant SHR increase from 5.28 °C min^{-1} to the maximum value 255.10 °C min^{-1} (at 274.9 °C).

In Fig. 4, both the pressure and pressure change rate as function of time indicated that the pressure of reaction system had two different stages and the turning point occurred at 240 °C. At the first stage where the temperature was below 240 °C, the pressure rise rate increased slowly due to the presence of small amount of gaseous products produced by the slow decomposition of TEX. At the second stage when the temperature exceeded 240 °C, the pressure rise rate increased suddenly because the rapid decomposition of DNTF occurred and yielded large amount of gaseous products such as NO_2, CO_2, N_2O, CO, NO, HCN, HCHO, and HNCO [28]. Figure 5 demonstrates that longer time was needed to reach the maximum temperature rise rate at lower initial heating temperature in the thermal decomposition reaction of TEX under adiabatic condition.

Data correction

Under experimental conditions of ARC, heat from the exothermic reaction of the sample induced the temperature rise of both sample and reaction bomb. The relationship between the real adiabatic and near adiabatic condition was described as following.

$$M_s C_{v,s} m_T = \left[(M_s C_{v,s} + M_b C_{v,b})\right] m_T \tag{1}$$

where M_s is the mass of the reactive sample, $C_{v,s}$ is the heat capacity of reaction sample, M_b is the mass of the reaction bomb, $C_{v,b}$ is the heat capacity of reaction bomb, and m_T is the self-heat rate of the reaction system including the reactive sample and the reaction bomb.

Hence, in order to obtain the data of the sample itself under the absolute adiabatic condition, it is necessary to correct the tested temperature parameters such as the adiabatic temperature rise, temperature rise rate, and the time of maximum temperature rise rate using the thermal inertia factor (Φ) to exclude the effect from reaction bomb, which was defined as following [20]:

$$\Phi = 1 + \frac{M_b C_{v,b}}{M_s C_{v,s}} \tag{2}$$

$$T_{0,s} = \left[\frac{1}{T_0} + \frac{R}{E_a}\ln\Phi\right]^{-1} \tag{3}$$

$$T_f = \Phi\Delta T_{ad} + T_{0,s} \tag{4}$$

$$\Delta T_{ad} = \Phi\Delta T_{ad,s} \tag{5}$$

$$m_{0,s} = \Phi m_0 \tag{6}$$

$$m_{m,s} = \Phi m_m \tag{7}$$

$$T_{m,s} = T_{0,s} + \Phi(T_m - T_0) \tag{8}$$

$$\theta_{m,s} = \frac{\theta_m}{\Phi} \tag{9}$$

where $T_{0,s}$ is the corrected initial decomposition temperature; T_f is the corrected final decomposition temperature; T_{ad} is the corrected adiabatic temperature rise; m_o is the corrected initial temperature rise; m_m is the corrected maximum temperature rise; T_m is the corrected temperature of maximum temperature rise rate; and θ_m is the corrected time of maximum temperature rise rate.

Kinetic parameters calculation

For an *n*th-order reaction with a single reaction, the SHR of adiabatic system could be expressed as the following:

$$k^* = C_0^{n-1} k = \frac{m_T}{\Delta T_{ad}\left[\frac{T_f - T}{\Delta T_{ad}}\right]^n} \tag{10}$$

where m_T is the SHR at arbitrary temperature *T* of adiabatic system; ΔT_{ad} is the measured adiabatic temperature rise; T_f is the measured final decomposition temperature; and k^* is a pseudo-zero-order rate constant at temperature *T*. According to the Arrhenius equation $k = A\exp(-E_a/RT)$, one can obtain:

Table 4 Kinetic parameters of TEX adiabatic decomposition

n	R^2	A/s^{n-1}	E_a/kJ mol^{-1}
0	0.99598	2.47×10^{26}	306.67
0.5	0.99369	1.73×10^{31}	353.21
1	0.99148	1.22×10^{36}	399.75
2	0.98763	5.95×10^{45}	492.84

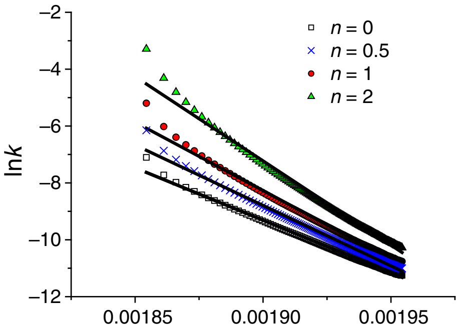

Fig. 6 Curve of ln*k* to 1/*T* for the decomposition of TEX

$$\ln k^* = \ln C_0^{n-1} A - \frac{E_a}{R}\left[\frac{1}{T}\right] \tag{11}$$

The plot of lnk^* versus 1/*T* is, therefore, expected to be a straight line providing that the order of reaction was correctly chosen. The regarding linear coefficient R^2, pre-exponential factor A, and the apparent activated energy E_a are listed in Table 4, and the curves between ln*k* and 1/*T* for the decomposition of TEX are illustrated in Fig. 6.

5-Second delay exploding point calculation

According to the literature [29], time to maximum temperature, E_a, and *A* have the relationship as follows:

$$\ln\theta = \frac{E}{R} \times \frac{1}{T} - \ln A \tag{12}$$

From Table 3, *E* and *A* were given as 306.67 kJ mol^{-1} and 2.47×10^{26} s^{-1}, respectively. Then, the 5-s delay exploding point could be calculated by above equation to be 318.15 °C, which is lower than the data (343 °C) [30] obtained by the traditional Wood's alloy bathy method.

Conclusions

The thermal decomposition behaviors and the thermal hazard assessment of TEX were first time exploited by using ARC. The results suggested that the standard molar specific heat capacity of TEX is 0.9038 J g^{-1} K^{-1} at 298.15 K, and the equation describing values of the capacity versus temperature was obtained to be $C_p = 0.81806 + 0.00341 \times T$, 5.0 °C $\leq T \leq$ 35 °C. Moreover, from the ARC data, it is suggested that the initial exothermic temperature was 215.8 °C under the adiabatic condition. In addition, the E_a, A, and 5-s delay exploding point of TEX were also given.

References

1. Sikder AK, Sikder N. A review of advanced high performance, insensitive and thermally stable energetic materials emerging for military and space applications. J Hazard Mater. 2004;112:1–15.
2. Millar RW, Philbin SP, Claridge RP, Hamid J. Studies of novel heterocyclic insensitive high explosive compounds: pyridines, pyrimidines, pyrazines and their bicyclic analogues. Propellants, Explos, Pyrotech. 2004;29:81–92.
3. Chapman RD, Wilson WS, Fronabarger JW, Merwin LH, Ostrom GS. Prospects of fused polycyclic nitroazines as thermally insensitive energetic materials. Thermochim Acta. 2002;384: 229–43.
4. Singh RP, Verma RD, Meshri DT, Shreeve JM. Energetic nitrogen-rich salts and ionic liquids. Angew Chem Int Ed. 2006;45:3584–601.
5. Zhu J, Jin S, Wan L, Zhang C, Li L, Chen S, Shu Q. Nitrogen-rich 4,4′-azo bis(1,2,4-triazolone) salts—the synthesis and promising properties of a new family of high-density insensitive materials. Dalton Trans. 2016;45:3590–8.
6. Zhang J, Shreeve JM. 3,3′-initroamino-4,4′-zoxyfurazan and its derivatives: an assembly of diverse N–O building blocks for high-performance energetic materials. J Am Chem Soc. 2014;136:4437–45.
7. Thottempudi V, Yin P, Zhang J, Parrish DA, Shreeve JM. 1,2,3-triazolo[4,5,-e]furazano[3,4,-b]pyrazine 6-oxide—a fused heterocycle with a roving hydrogen forms a new class of insensitive energetic materials. Chem Eur J. 2014;20:542–8.
8. Gao H, Shreeve JM. Azole-based energetic salts. Chem Rev. 2011;111:7377–436.
9. Thottempudi V, Gao H, Shreeve JM. Trinitromethyl-substituted 5-nitro- or 3-azo-1,2,4-triazoles: synthesis, characterization, and energetic properties. J Am Chem Soc. 2011;133:6464–71.
10. Wang R, Xu H, Guo Y, Sa R, Shreeve JM. Bis[3-(5-nitroimino-1,2,4-triazolate)]-based energetic salts: synthesis and promising properties of a new family of high-density insensitive materials. J Am Chem Soc. 2010;132:11904–5.
11. Fischer N, Fischer D, Klapötke TM, Piercey DG, Stierstorfer J. Pushing the limits of energetic materials—the synthesis and characterization of dihydroxylammonium 5,5′-bistetrazole-1,1′-diolate. J Mater Chem. 2012;22:20418–22.
12. Dippold AA, Klapötke TM. A study of dinitro-bis-1,2,4-triazole-1,1′-diol and derivatives: design of high-performance insensitive energetic materials by the introduction of N-Oxides. J Am Chem Soc. 2013;135:9931–8.
13. Koch EC. TEX-4,10-dinitro-2,6,8,12-tetrapxa-4.10-diazatetracyclo[5.5.0.0.^{5,9}.0$^{3.11}$]-dodecane-review of a promising high density insensitive energetic material. Propellants, Explos, Pyrotech. 2015;40:374–87.
14. Xiao LB, Zhao FQ, Luo Y, Gao HX, Li N, Meng ZH, Hu RZ. Thermal behavior and safety of 4,10-dinitro- 2,6,8,12-tetrapxa-4.10-diazaisowutrzitane. J Therm Anal Calorim. 2015;121: 839–42.
15. Lei YP, Xu SL, Yang SQ, Zhang T. Progress in high energetic explosive: TEX. Chin J Energ Mater. 2006;6:467–70.
16. Vagenknecht J. TEX—a lova explosive. Chin J Energ Mater. 2008;8:56–9.
17. Vagenknecht J, Marecek P, Trzcinski W. Sensitivity and performance properties of TEX explosive. J Energ Mater. 2002;20:245–53.
18. Wang R, Meng ZH, Xue M, Xu ZB, Cui KJ, Zhao FQ, Xiao LB, Guo Q. Compatibility of high energetic explosive TEX with components of propellants by DSC method. Chin J Explos Propellants. 2015;38:66–9.
19. Li YC, Yan S, Cheng Y. Thermal decomposition kinetics of RDX by TG-DSC-QMS-FTIR. Chin J Explos Propellants. 2009; 32:32–5.
20. Tang Z, Yang L, Qiao XJ, Zhang TL, Yu WF. On thermal decomposition kinetics and thermal safety of HMX. Chin J Energ Mater. 2011;19:396–400.
21. Fung V, Morris J, Price D, Tucker N, Claire EL, Carrillo A. Further development and optimization of IM ingredients at Holston army ammunition plant. In: Insensitive munitions and energetic materials technology symposium. Munich, Germany; 2010.
22. Zeng XL, Ju XH, Gao HX. Theoretical study of 4,10-dinitro-2,6,8,12-tetraoxa-4,10-diaza-tetracyclododecane (TEX). Adv Mater Res. 2012;554–556:1618–23.
23. Townsend DI, Tou JC. Thermal hazard evaluation by an accelerating rate calorimeter. Thermochim Acta. 1980;37:1–30.
24. Tou JC, Whiting LF. The thermokinetic performance of an accelerating rate calorimeter. Thermochim Acta. 1981;48:21–42.
25. Lu KT, Yang CC, Lin PC. The criteria of critical runaway and stable temperatures of catalytic decomposition of hydrogen peroxide in the presence of hydrochloric acid. J Hazard Mater. 2006;135:319–27.
26. Fu ZM, Koseki H, Iwata Y. Investigation on thermal stability of flavianic acid disodium salt. J Loss Prevent Proc. 2009;22:477–83.
27. Liu HP, Gu LY, Zhu P, Liu ZR, Zhou B. Effect of micro amount of Fe^{3+} on thermal explosion decomposition of hydrogen peroxide. Fire Sci Tech. 2012;31:554–7.
28. Zuo YF, Chang K, Chen J, Cheng KM, Wang XF, Fang YX. Characteristics of thermal decomposition of TEX. Chin J Energ Mater. 2006;14:387–8.
29. Liu Y, Yang Q, Chen LP, He ZQ, Lu Y, Chen WH. Thermal sensitivity of energetic materials characterized by accelerating rate calorimeter (ARC). Chin J Energ Mater. 2011;19:656–60.
30. Zuo YF, Xu R, Chang K, Peng Q, Liu JB. Influence of RDX and HMX on the thermal stability of TEX. J Energ Mater. 2005;13:110–2.